Remote Plasma-Enhanced Chemical Vapor Deposited a-SiS_x:H. Characterization by Raman and Solid-State NMR Spectroscopies and Relationship to the Structure of Vitreous SiS_2

R. K. Shibao, V. I. Srdanov, M. Hay, and H. Eckert*

Department of Chemistry, University of California, Santa Barbara, California 93106

Received September 14, 1993. Revised Manuscript Received December 10, 1993®

Amorphous SiS_x:H ($x \sim 2$) films have been synthesized, for the first time, from molecular H_2S and SiH_4 precursors, using a remote plasma-enhanced chemical vapor deposition apparatus. Structural studies by solid-state nuclear magnetic resonance and Raman scattering reveal that the atomic environments in these materials are similar to those observed in melt-quenched silicon sulfide glasses and are characterized by corner- and edge-shared $SiS_{4/2}$ tetrahedra. Compared to these glasses, however, the films show consistently higher fractions of corner-sharing $SiS_{4/2}$ tetrahedra. The ratio of corner- to edge-sharing tetrahedra and the Si:S ratio can be influenced by the H_2S/SiH_4 flow rate ratio during deposition. Thus, PECVD opens up wider opportunities for structural tailoring of amorphous silicon sulfide materials than currently possible by means of the melt-quenching method.

Introduction

Non-oxide chalcogenide glasses based on the sulfides, selenides, and tellurides of main-group elements are solid-state materials of both technological and fundamental scientific interest.[1] Glassy SiS_2, $SiSe_2$, B_2S_3, and P_2S_5 form the base materials for a novel class of vitreous fast Li ion conductors with promise for solid-state battery applications.[2,3] They are also potentially useful in applications for infrared-transparent fibers and films.[4,5] From a scientific point of view, these amorphous homologues of glass-forming oxides are intriguing model systems to investigate fundamental questions concerning glass structure, a subject of much current interest. Most recently, such studies have produced intricate detail and structural insights into chalcogenide glasses, which frequently contradict longheld traditional views and concepts of glass structure.[6,7]

One of the general technological benefits of glasses (as opposed to crystalline compounds) is the opportunity of altering the physical properties of a chemical system in a continuous manner through compositional variation. In many oxide systems, nontraditional synthesis routes (sol–gel, chemical vapor deposition, etc.) have proven very useful for preparing homogeneous glasses in systems that would normally phase-separate under high-temperature melt conditions. In contrast to the situation for oxide glass systems, however, previous applications of nontraditional synthesis routes for non-oxide chalcogenide glasses have been been extremely limited. The few accounts in the literature include the preparation of glassy As_2S_3 by solution-state processing[8] and vapor deposition methods[9] and the use of plasma-enhanced chemical vapor deposition for the preparation of amorphous $GeSe_2$ films.[10-12]

This contribution reports the nontraditional synthesis of amorphous materials in the silicon–sulfur system. This system is of fundamental interest, because bulk SiS_2 and $SiSe_2$ glasses are known to violate the Zachariasen rule[13] that the preferred connectivity mode in covalent glasses is exclusively via corner-sharing tetrahedra. Rather, previous Raman[14-19] and solid-state NMR studies[20,21] have shown unequivocally that the glasses are composed of both corner- and edge-shared $SiX_{4/2}$ (X = S, Se) tetrahedra in a fairly constant ratio. In addition, Raman studies have revealed that silicon sulfide glasses with higher sulfur contents tend to segregate into elemental sulfur plus a glassy phase with a structural speciation similar to that in glassy SiS_2.[22] On the basis of these results, traditional melt-quenching techniques offer essentially no opportunities for any structural or compositional tailoring. In the present contribution we report the first preparation of amorphous silicon sulfide films by using plasma-enhanced

* Abstract published in *Advance ACS Abstracts*, February 1, 1994.

(1) Taylor, P. C. *Mater. Res. Soc. Bull.* **1987**, 36.
(2) Pradel, A.; Ribes, M. *Solid State Ionics* **1986**, *18/19*, 351.
(3) Kennedy, J. H.; Zhang, Z.; Eckert, H. *J. Non-Cryst. Solids* **1990**, *123*, 328.
(4) Churbanov, M. F. *J. Non-Cryst. Solids* **1992**, *140*, 324.
(5) Nishii, J.; Morimoto, S.; Inagawa, I.; Iizuka, R.; Yamishita, T.; Yamagashi, T. *J. Non-Cryst. Solids* **1992**, *140*, 199.
(6) Elliott, S. R. *Nature* **1991**, *354*, 445.
(7) Eckert, H. *Prog. Nucl. Magn. Reson. Spectrosc.* **1992**, *24*, 159.
(8) Guiton, T. A.; Pantano, C. G. *Chem. Mater.* **1989**, *1*, 558.
(9) DeNeufville, J. P.; Moss, S. C.; Ovshinsky, S. R. *J. Non-Cryst. Solids* **1974**, *13*, 191.
(10) Ribes, M.; Cros, B.; Peytavin, S.; Camon, H.; Balladore, J. L. *Mater. Res. Soc. Symp. Proc.* **1990**, *165*, 233.
(11) Cros, B.; Brocheton, Y.; Ribes, M. *Mater. Manufactoring Processes* **1990**, *5*, 411.
(12) Tick, P. A.; Wallace, N. W.; Teter, M. P. *J. Vac. Sci. Technol.* **1974**, *11*, 709.
(13) Zachariasen, W. W. *J. Am. Ceram. Soc.* **1932**, *54*, 3841.
(14) Tenhover, M.; Hazle, M. A.; Grasselli, R. K. *Phys. Rev. Lett.* **1983**, *51*, 404.
(15) Tenhover, M.; Hazle, M. A.; Grasselli, R. K.; Tompson, C. W. *Phys. Rev. B* **1983**, *28*, 4608.
(16) Tenhover, M.; Henderson, R. S.; Lukco, D.; Hazle, M. A.; Grasselli, R. K. *Solid State Commun.* **1984**, *51*, 455.
(17) Sugai, S. *Phys. Rev. B* **1987**, *35*, 1345.
(18) Griffiths, J. E.; Malyi, M.; Espinosa, P.; Remeika, J. P. *Phys. Rev. B* **1984**, *30*, 6978.
(19) Tenhover, M.; Harris, J. H.; Hazle, M. A.; Scher, H.; Grasselli, R. K. *J. Non-Cryst. Solids* **1985**, *69*, 249.
(20) Tenhover, M.; Boyer, R. D.; Henderson, R. S.; Hammond, T. F.; Schreve, G. A. *Solid State Commun.* **1988**, *65*, 1517.
(21) Moran, K.; Shibao, R.; Eckert, H. *Hyperfine Interact.* **1990**, *62*, 55.
(22) Tenhover, M.; Henderson, R. S.; Hazle, M. A.; Lukco, D.; Grasselli, R. K. *Design of New Materials*; Cocke, D., Clearfield, A., Eds.; Plenum Publishing: New York, 1987; p 329.

0897-4756/94/2806-0306$04.50/0

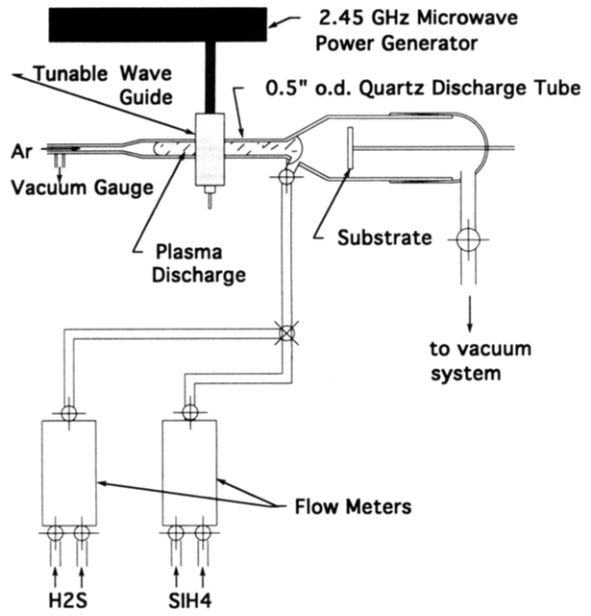

Figure 1. Schematic of the PECVD apparatus developed during the present study.

chemical vapor deposition (PECVD) methods,[23] and the structural characterization of these films by spectroscopic methods. Attention will be paid to the questions of whether the PECVD method produces materials that are structurally substantially different from bulk melt-quenched glasses and whether phase segregation off-stoichiometry with respect to SiS_2 can be avoided. Our studies, which focus on the chalcogen-rich side of the composition diagram, are complementary to the work of other groups, who have reported on sulfur-doped a-Si:H films with sulfur concentrations up to a maximum of 25 at. %.[24-29]

Experimental Section

Sample Preparation. Bulk amorphous silicon sulfide was prepared from the elements using standard literature procedures.[14-19] The a-SiS_x:H samples were synthesized using the remote plasma-enhanced chemical vapor deposition (RPECVD) apparatus shown schematically in Figure 1. The deposition chamber and the discharge tube are constructed of fused silica, 2.5-in.-o.d., 10-in. length, and 0.5-in.-o.d., 11-in. length, respectively. In a typical deposition run an argon (Liquid Carbonic, chromatography grade) plasma was sustained (p_{Ar} = 300–600 mTorr) with a 2.45–GHz Raytheon microwave power generator. Silane (Liquid Carbonic, semiconductor grade) mixed with hydrogen sulfide (Aldrich, 99.5+%) was introduced into the downstream tail of this plasma. The apparatus and the substrate were not externally heated, and the samples were deposited directly on the walls and on an aluminum foil substrate positioned 0.5–3 cm downstream of the plasma tail. Deposition parameters are listed in Table 1. The silicon/sulfur ratios were altered by adjustment of the H_2S/SiH_4 flow rate ratio within the range 1–3. Lower ratios produce materials similar to a-Si:H, while higher flow rate ratios lead to the production of excess sulfur in addition to markedly decreased deposition rates. The deposits appeared visually homogeneous and ranged from reddish to white in color, lighter colors being associated with higher H_2S/SiH_4 flow rate ratios. The films are extremely unstable in ambient atmospheric conditions and are hydrolyzed rapidly by moisture, forming H_2S. Therefore, all sample handling and storage were done in a stainless steel glovebox sustaining a dry helium atmosphere with water levels less than 1 ppm.

Table 1. Representative Deposition Parameters for Amorphous SiS_x:H Films, Results from Chemical Analysis, and $E^{(n)}$ Speciation from ^{29}Si MAS NMR

deposition pressure P_{tot}, mTorr	510	450	
deposition rate, mg/h	65	35	
flow rates, sccm			
SiH_4	100	150	melt-quenched
H_2S	300	300	a-SiS_2
MW power, W	64	64	
wt. % Si	27.1	35.3	31.3
wt. % H	<0.5	<0.5	<0.5
calcd stoichiometry	$SiS_{2.3}$	$SiS_{1.6}$	$SiS_{2.0}$
$E^{(0)}:E^{(1)}:E^{(2)}$	29:50:21 (±2)	45:38:17 (±4)	13:48:39 (±2)

Characterization. X-ray powder diffraction, carried out on a Scintag diffractometer using Cu Kα radiation, confirmed the totally amorphous character of all of the SiS_x:H films prepared. Differential scanning calorimetry, carried out on a duPont 912 system, indicated the absence of thermal events attributable to SiS_2 over the temperature range $50 \le T \le 500$ °C. However, certain samples reveal several unresolved endothermic transitions within the temperature range 90 °C $\le T \le$ 120 °C, consistent with the presence of elemental sulfur. Chemical analysis (performed by Galbraith Laboratories) gave the results listed in Table 1. These values were reproducible in replicate runs. For comparison, chemical analysis of a sample of amorphous SiS_2, produced by melt quenching, yielded 31.3 wt % Si (expected 30.5 wt.%) and <0.5 wt % H. The chemical analysis results reveal that the H/Si ratio lies below 0.8 and that the Si/S ratio of these films can be varied by the flow rate ratio in the expected manner. Attempts to quantitate the hydrogen content by ^1H NMR gave irreproducible results, due to large proton background contributions in the NMR probe. Also, IR spectra obtained on KBr pellets showed no clear manifestations of either Si–H or S–H bonds.

Raman spectra were recorded in a backscattering geometry using liquid nitrogen cooled 2D CCD detector (Princeton Instruments Model LN/CCD-1152/UV) attached to a fast f/6.9 0.5-m monochromator (Acton Research Model Spectra Pro-500) equipped with 600 grooves/mm grating blazed at 500 nm. Approximately 5 mJ/pulse at 10 Hz of the 532-nm radiation generated by a Nd:YAG laser (Quanta Ray DCR-11) was softly focused onto the capillary Pyrex tube containing powdered sample. A Raman holographic edge filter (Physical Optics Corporation Model RHE 532.10) placed in front of the entrance slit of the monochromator provided overall 10^{-10} stray light rejection factor at 300 cm^{-1} from the Rayleigh line. Typical exposure time was 15 s. The accuracy of the measurements was better than 2 cm^{-1}.

^{29}Si magic-angle spinning (MAS) and ^1H–^{29}Si cross-polarization magic angle spinning (CPMAS) NMR experiments were carried out at 59.7 MHz on a General Electric GN-300 spectrometer, equipped with a 7-mm multinuclear MAS-NMR probe from Doty Scientific and at 99.06 MHz on a Chemagnetics CMX 500 NMR spectrometer utilizing different contact times ranging from 2 to 20 ms. The following typical experimental conditions were used for ^{29}Si MAS NMR, in accordance with previous studies:[20,21] spinning speeds 3–6 kHz, 90° pulses of 8–10-μs length, relaxation delay 1 h. Experiments with variable relaxation delays (up to 3 h) showed that these conditions result in representative peak area ratios, and that at least ca. 80% of the Si atoms are fully relaxed. ^1H MAS NMR spectra were recorded on a General Electric GN-300 spectrometer at 300.56 MHz, using spinning speeds of 6–8 kHz, 2-μs pulse lengths, and relaxation delays of 4–8 min.

(23) For a general review of RPECVD techniques, see: Rossnagel, S. M.; Cuomo, J. J.; Westwood, W. D. *Handbook of Plasma Processing Technologies*; Noyes Publications: Park Ridge, NY.
(24) Lin, G. H.; Kapur, M.; He, M. Z.; Bockris, J. O. M. *J. Non-Cryst. Solids* **1991**, *127*, 186.
(25) Al-Dallal, S.; Hammam, M.; Al-Alawi, S. M.; Aljishi, S.; Breitschwerdt, A. *Philos. Mag. B* **1991**, *63*, 839.
(26) Al-Dallal, S.; Aljishi, S.; Hammam, M.; Al-Alawi, A. M.; Stutzmann, M.; Jin, S.; Mushik, T.; Schwarz, R. *J. Appl. Phys.* **1991**, *70*, 4926.
(27) Al-Dallal, S.; Hammam, M.; Al-Alawi, A. *J. Non-Cryst. Solids* **1989**, *114*, 462, 789.
(28) He, M. Z.; Lin, G. H.; Bockris, J. O. M. *J. Non-Cryst. Solids* **1992**, *142*, 108.
(29) Lin, G. H.; Kapur, M.; Bockris, J. O. M. *Solar Energy Mater. Sol. Cells* **1992**, *28*, 29.

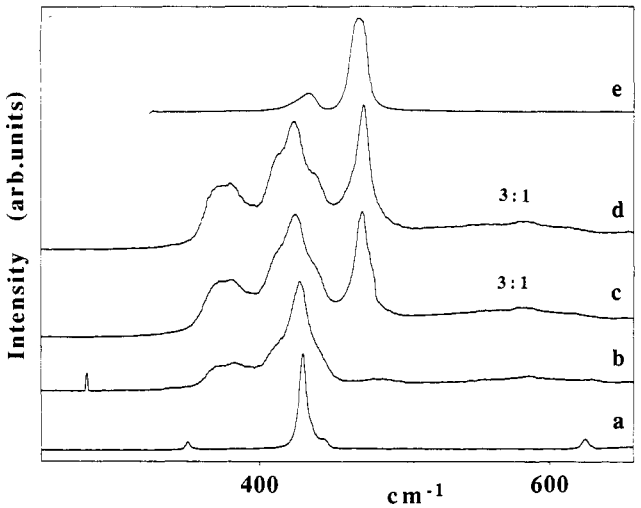

Figure 2. Raman spectra of (a) crystalline SiS_2; (b) bulk SiS_2 glass; (c) SiS_x:H film deposit, using SiH_4 flow rate 100 sccm, H_2S flow rate 300 sccm, P_{tot} 500 mTorr, 64 W; (d) SiS_x:H film deposit, using SiH_4 flow rate 60 sccm, H_2S flow rate 180 sccm, P_{tot} 420 mTorr, 56 W; (e) elemental sulfur. H_2S/SiH_4 flow rate ratios are indicated.

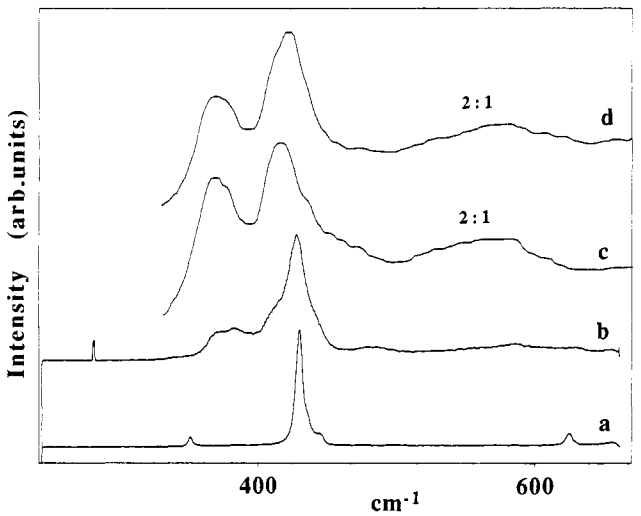

Figure 3. Raman spectra of (a) crystalline SiS_2; (b) bulk SiS_2 glass; (c) SiS_x:H film deposit, using SiH_4 flow rate 150 sccm, H_2S flow rate 300 sccm, P_{tot} 740 mTorr, 64 W; (d) SiS_x:H film deposit, using SiH_4 flow rate 150 sccm, H_2S flow rate 300 sccm, P_{tot} 450 mTorr, 64 W. H_2S/SiH_4 flow rate ratios are indicated.

Results and Discussion

Raman Spectroscopy. Figures 2 and 3 compare the Raman spectra of representative samples to those of elemental sulfur and crystalline and glassy SiS_2. The Raman spectrum of glassy SiS_2 is identical with that already reported and discussed in detail in the literature;[14-19,22] the most reliable assignments are discussed in detail in ref 22. The spectrum is dominated by two intense and structured peaks at 425 and 380 cm^{-1}. Of these, only the 425-cm^{-1} peak is observed in crystalline SiS_2 and reflects a mode associated with the A_1 vibrations of edge-sharing tetrahedra, whereas the peak near 380 cm^{-1} arises from the A_1 vibrations of corner-sharing tetrahedra. Previous studies of sulfur-rich bulk nonstoichiometric SiS_x glasses have shown that the 425/380 cm^{-1} peak ratio is essentially unchanged, and a new intense peak emerges at 470 cm^{-1}, which is easily assigned to the A_1 mode of S_8. The 470-cm^{-1} peak is further accompanied by a weaker feature at 440 cm^{-1} which partially overlaps the 425-cm^{-1} band, and is also attributed to S_8. On the basis of these observations, Tenhover *et al.* concluded that SiS_x ($x > 2$) glasses phase separate into stoichiometric amorphous SiS_2 and elemental sulfur.[22]

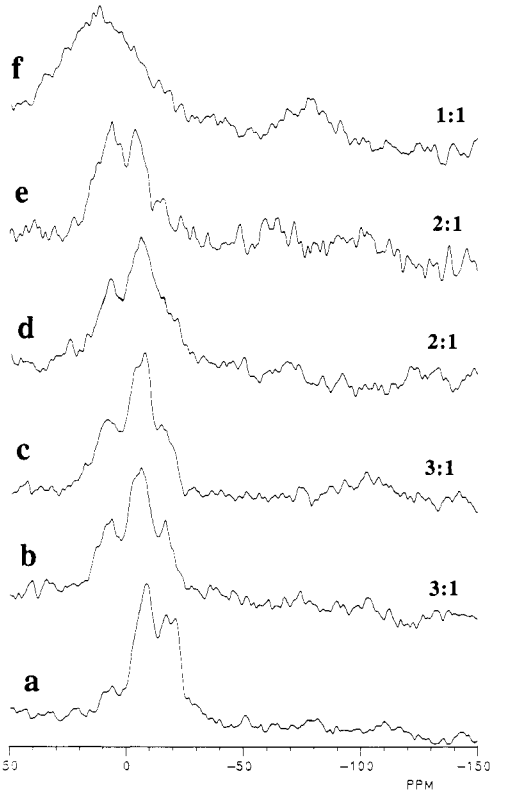

Figure 4. The 59.7-MHz ^{29}Si MAS NMR spectra of (a) bulk SiS_2 glass; (b) SiS_x:H film deposit, using SiH_4 flow rate 100 sccm, H_2S flow rate 300 sccm, P_{tot} 500 mTorr, 64 W; (c) SiS_x:H film deposit, using SiH_4 flow rate 60 sccm, H_2S flow rate 180 sccm, P_{tot} 420 mTorr, 56 W; (d) SiS_x:H film deposit, using SiH_4 flow rate 150 sccm, H_2S flow rate 300 sccm, P_{tot} 450 mTorr, 64 W; (e) SiS_x:H film deposit, using SiH_4 flow rate 150 sccm, H_2S flow rate 300 sccm, P_{tot} 740 mTorr, microwave power 64 W; (f) a-SiS_x:H film deposit, using H_2S and SiH_4 flow rates 150 sccm, P_{tot} 500 mTorr, 64 W. H_2S/SiH_4 flow rate ratios are indicated.

The Raman spectra obtained on the PECVD-generated samples show essentially the same peaks, albeit slightly shifted. The peak intensity ratios, however, are significantly different from that in bulk SiS_2 glass, suggesting a larger fraction of corner-sharing $SiS_{4/2}$ tetrahedra in the films as compared to the bulk glass. In addition to these two Si–S modes, the A_1 mode attributed to elemental sulfur is observed, but only in the SiS_x films generated with H_2S/SiH_4 flow rate ratios ≥3:1. Overall, both Figures 2 and 3 indicate that the rate of film growth, which is largely governed by the absolute flow rates of the gaseous reactants and the deposition pressure used has fairly little influence on the microstructure, at least within the ranges explored here. In contrast, comparison of Figure 2 with Figure 3 illustrates that the H_2S/SiH_4 flow rate ratio is a decisive parameter for structural control. Again, this situation is different from that in the molten state, where changes in the silicon/sulfur melt composition just produce different relative amounts of segregated phases.

^{29}Si MAS NMR. Figure 4 shows the ^{29}Si MAS NMR spectroscopic results. As previously observed for bulk Si–S glasses,[20,21] the ^{29}Si spin lattice relaxation times in the film deposits are extremely long, necessitating the use of ≥1-h relaxation delays; this explains the generally poor signal-to-noise ratios. All of the spectra show negligible signal intensity upfield of −30 ppm (except for a contri-

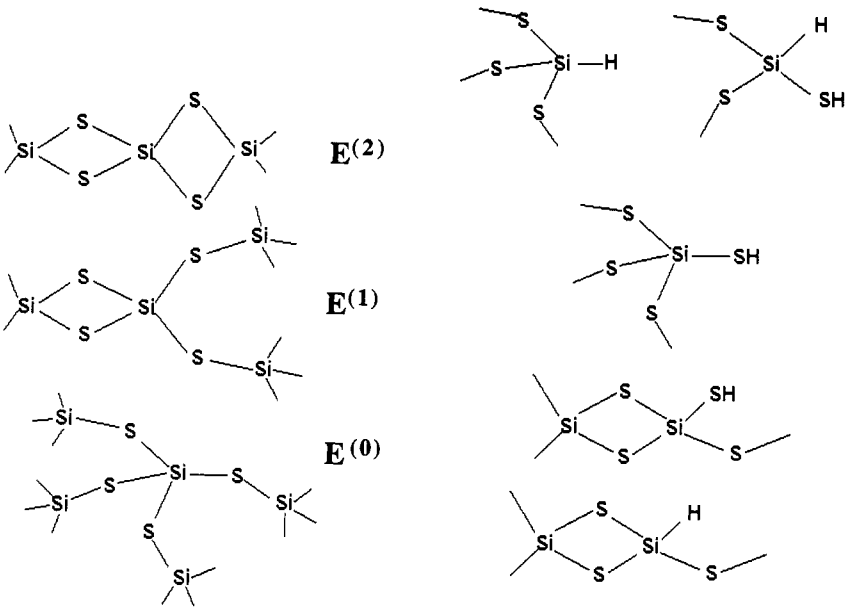

Figure 5. (a, left) $E^{(0)}$, $E^{(1)}$, and $E^{(2)}$ sites in silicon sulfide glasses and films, as inferred from ^{29}Si MAS NMR. (b, right) Possible sites involving hydrogen species in SiS$_x$:H films.

bution from Si–H groups at −80 ppm), revealing that contamination with oxygen if present is structurally insignificant. The NMR spectrum of glassy SiS_2 corresponds to that already discussed in the literature.[12,13] The three main signal components centered near 7, −7, and −19 ppm are assigned to $E^{(0)}$, $E^{(1)}$, and $E^{(2)}$ units, respectively. As illustrated in Figure 5a, the symbol $E^{(0)}$ denotes corner-shared $SiS_{4/2}$ tetrahedra, $E^{(1)}$ denotes $SiS_{4/2}$ units sharing one common edge with an adjacent tetrahedron and linked to two other $SiS_{4/2}$ units by corner-sharing, and $E^{(2)}$ denotes $SiS_{4/2}$ units sharing edges with two adjacent tetrahedra. Closer inspection of Figure 4a reveals that the $E^{(2)}$ resonance is split into two components at −17 and −21 ppm. Crystalline SiS_2 is composed exclusively of $E^{(2)}$ units, which form one-dimensional chains[30,31] and gives a single resonance at −21.1 ppm.[20,21] Thus the −21 ppm resonance in the glass is assigned to Si atoms within longer chains, where $E^{(2)}$ units are adjacent to only other $E^{(2)}$ units. In contrast, the −17 ppm resonance is tentatively assigned to $E^{(2)}$ units that are parts of smaller chain fragments where $E^{(2)}$ units are adjacent to $E^{(1)}$ units. In a similar fashion to $E^{(1)}$ signal around −7 ppm appears to be split into two components around −4 and −9 ppm, respectively. Again, the chemical shift discrimination might arise from adjacent $E^{(1)}$ or $E^{(2)}$ species, although no firm assignments can be made at this time. A recent study of two new low-temperature forms of $SiSe_2$ has shown that ^{29}Si chemical shifts are quite sensitive to such next-nearest-neighbor bonding effects.[32]

The ^{29}Si NMR spectra of the RPECVD grown films illustrate the crucial influence of the H_2S/SiH_4 flow rate ratio on the film microstructure. Spectra obtained for the samples with a 3:1 flow rate ratio closely resemble those of melt-quenched SiS_2, confirming the structural similarities between both types of materials. Excellent reproducibility is observed for different separate preparations. The NMR spectra suggest, however, consistent with the Raman data, that the fraction of corner-sharing tetrahedra in the films is significantly higher in the vapor deposits. Since under equilibrium conditions the NMR signal intensities are directly related to the number of nuclei giving rise to this signal, we can arrive at approximate $E^{(n)}$ concentrations as listed in Table 1. On the basis of these NMR and Raman data, the RPECVD samples have reduced concentrations of $E^{(2)}$ environments, while the fraction of $E^{(0)}$ units is substantially enhanced. These spectra also show the same fine structure for the $E^{(1)}$ and $E^{(2)}$ sites and suggest that the number of long chain units in the vapor deposits is lower than in the bulk glass. For samples prepared with a 2:1 H_2S/SiH_4 flow rate ratio the fraction of $E^{(0)}$ units is increased even further, and again excellent reproducibility is observed. Finally, in samples prepared with a 1:1 H_2S/SiH_4 flow rate ratio, the spectral resolution in the region attributable to S-bonded silicon is lost and a distinct signal component around −80 ppm emerges, revealing the formation of a-Si:H islands.

^{1}H–^{29}Si CPMAS and ^{1}H MAS NMR. A likely explanation for the increased $E^{(0)}$ content with decreasing H_2S/SiH_4 flow rate ratio is the structural incorporation of hydrogen atoms, which might be present in the form of "defect" units such as shown in Figure 5b. Figure 6 reveals that it is possible to cross-polarize the Si sites from hydrogen, revealing structural proximity between Si and H atoms. The CPMAS NMR spectra of samples generated with a 3:1 flow rate ratio are qualitatively similar to the results from ^{29}Si single-pulse NMR but do show moderately enhanced signal intensities for the $E^{(0)}$ units. In contrast, the CPMAS spectra of the samples generated with a 2:1 flow rate ratio are fundamentally different, possibly reflecting large defect concentrations and inhomogeneous hydrogen distributions. The spectrum shows four resonances centered near −2, −48, −80, and −105 ppm. Previous studies on amorphous hydrogenated Si:H films have shown wide ^{29}Si chemical shift ranges for these materials, encompassing the values obtained here for the latter three resonances.[33–35] On the basis of this information, the following tentative assignments are made: the resonances centered around −2 ppm are attributed to S-bonded Si atoms, possibly including $Si(SH)S_{3/2}$ groups, while the

(30) Zintl, E.; Loosen, K. *Z. Kristallogr.* **1933**, *2*, 35.
(31) Peters, J.; Krebs, B. *Acta Crystallogr.* **1982**, *B38*, 1270.
(32) Pradel, A.; Michel-Lledos, V.; Ribes, M.; Eckert, H. *Chem. Mater.* **1993**, *5*, 377.

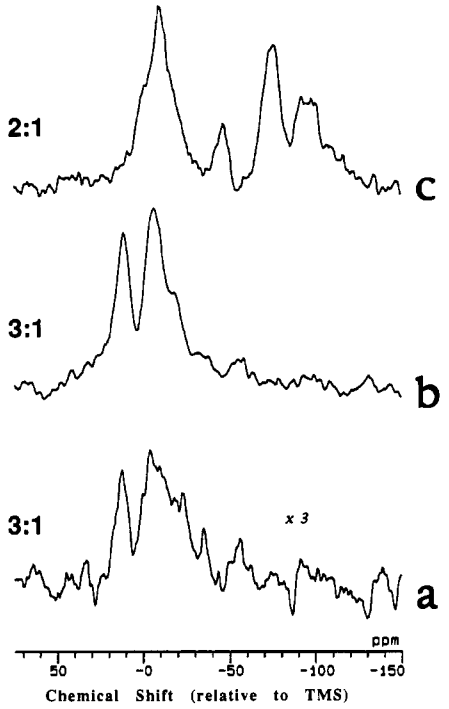

Figure 6. ^1H–^{29}Si CPMAS NMR spectra of SiS_x:H film deposits using (a) H_2S/SiH_4 flow rate ratio 3:1. CPMAS contact time 2 ms. (b) Same sample, CPMAS contact time 20 ms. (c) H_2S/SiH_4 flow rate ratio 2:1, CPMAS contact time 10 ms.

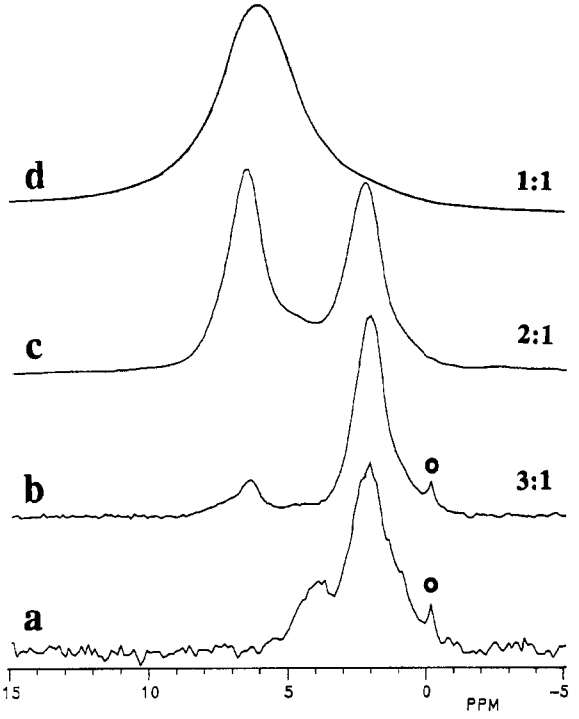

Figure 7. The 300.56-MHz ^1H MAS NMR spectra of (a) glassy SiS_2 obtained from melt-quenching; (b) SiS_x:H film deposit using H_2S/SiH_4 flow rate ratio 3:1; (c) SiS_x:H film deposit using H_2S/SiH_4 flow rate ratio 2:1; (d) SiS_x:H film deposit using SiH_4/H_2S flow rate ratio 1:1. Sharp lines marked with a circle are assigned to adsorbed molecular H_2S.

peaks around −48, −80, and −105 ppm are assigned to Si atoms bonded to hydrogen in various different environments resembling those present in a-Si:H. We cannot rule out that the peak at −105 ppm reflects silicon bonded to an OH group impurity. It must be emphasized that due to the relaxation dynamics involved in CPMAS NMR, the intensities of these four resonances are not representative of relative species concentrations. Comparison with the ^{29}Si single-pulse spectra shows that the defect silicon sites in the proximity of H atoms are greatly overestimated by the CPMAS method.

To clarify the situation further, additional information was sought from ^1H MAS NMR. The results are shown in Figure 7, revealing two well-resolved peaks at 6.4 and 2.0 ppm, respectively. The static ^1H NMR linewidth is around 5 kHz. The sharpness of the static and MAS NMR peaks indicates that the ^1H–^1H dipole–dipole interactions are fairly weak, suggesting that the hydrogen atoms are structurally isolated and not clustered. Extended sample annealing (4 h) at 190 °C in a 10^{-3} Torr vacuum produced no significant changes in the spectra. In view of these experiments, and further the fact that the ^{29}Si spins are easily cross-polarized from the hydrogen species, it is unlikely that the sharpness of the ^1H resonances arises from high atomic mobility. Figure 7 illustrates that the intensity ratio of the 6.4 and 2.0 ppm resonances is a systematic function of the H_2S/SiH_4 flow rate ratio under deposition conditions and thus of the S:Si ratio in the resulting film. On the basis of this compositional dependence, the peak at 6.4 ppm is assigned to silicon-bound H atoms, while the resonance at 2.0 ppm is attributable to terminal SH groups. Support for this assignment comes from additional experiments, which reveal that amorphous S_x deposited from remote PECVD of H_2S alone shows only the 2.0 ppm resonance. In addition, amorphous melt-quenched SiS_2 shows a very weak resonance at this shift, presumably arising from impurities (residual moisture) in the starting materials. Finally, exposure of the films to atmospheric moisture produces a narrow resonance at −0.1 ppm, probably due to surface-adsorbed hydrogen sulfide.

Conclusions

The preparation of amorphous SiS_x:H films by remote plasma-enhanced chemical vapor deposition (RPECVD) is reported for the first time. Variation of the flow rate ratio of the reagent gases H_2S and SiH_4 affords adjustment of the sulfur/silicon stoichiometry and also influences the structural speciation. Raman and ^{29}Si MAS NMR spectroscopies reveal that the structure of these films is based on $SiS_{4/2}$ tetrahedra that are interlinked both via corner and edge sharing. Compared to amorphous melt-quenched SiS_2, however, the fraction of corner-shared-only Si atoms is significantly enhanced in the films. ^1H–^{29}Si CPMAS experiments reveal that the Si atoms are in dipolar contact with H atoms, and ^1H MAS NMR studies indicate a distinction between Si- and S-bonded hydrogen species, both of which are structurally isolated and not clustered. The presence of such terminal hydrogen species is probably at least partially responsible for the altered structural speciation revealed by ^{29}Si NMR and Raman spectroscopy.

Acknowledgment. This work was supported by the National Science Foundation (Grants DMR 89-13738 and DMR 92-21197). We thank Dr. Ivo Kamber for assistance with the Raman measurements, Dr. Lucy Bull for help with the CPMAS NMR studies, and Mssrs. John McArthur, Brian Nadel, and Mark Beckert for assistance during construction of the deposition apparatus.

(33) Hayashi, S.; Hayamizu, K.; Yamasaki, S.; Matsuda, A.; Tanaka, K. *Phys. Rev. B* **1987**, *35*, 4581.
(34) Reimer, J. A.; Dubois Murphy, P.; Gerstein, B. C.; Knights, J. C. *J. Chem. Phys.* **1981**, *74*, 1501.
(35) Lamotte, B.; Rousseau, A.; Chenevas-Paule, A. *J. Phys.* **1981**, *42*, C4-839.